

A Polarimetric Search for Hidden Quasars in Three Radio Selected Ultraluminous Infrared Galaxies

Hien D. Tran¹, M. S. Brotherton¹, S. A. Stanford¹, Wil van Breugel¹, Arjun Dey², Daniel Stern³, Robert Antonucci⁴

ABSTRACT

We have carried out a spectropolarimetric search for hidden broad-line quasars in three ultraluminous infrared galaxies (ULIRGs) discovered in the positional correlations between sources detected in deep radio surveys and the *IRAS Faint Source Catalog*. Only the high-ionization Seyfert 2 galaxy TF J1736+1122 is highly polarized, displaying a broad-line spectrum visible in polarized light. The other two objects, TF J1020+6436 and FF J1614+3234, display spectra dominated by a population of young (A-type) stars similar to those of “E + A” galaxies. They are unpolarized, showing no sign of hidden broad-line regions. The presence of young starburst components in all three galaxies indicates that the ULIRG phenomenon encompasses both AGN and starburst activity, but the most energetic ULIRGs do not necessarily harbor “buried quasars”.

We find that a luminous infrared galaxy is most likely to host an obscured quasar if it exhibits a high-ionization ($[\text{O III}]\lambda 5007/\text{H}\beta \gtrsim 5$) spectrum typical of a “classic” Seyfert 2 galaxy with little or no Balmer absorption lines, is “ultraluminous” ($L_{\text{IR}} \gtrsim 10^{12} L_{\odot}$), and has a “warm” IR color ($f_{25}/f_{60} \gtrsim 0.25$). The detection of hidden quasars in this group but not in the low-ionization, starburst-dominated ULIRGs (classified as LINERs or H II galaxies) may indicate an evolutionary connection, with the latter being found in younger systems.

Subject headings: galaxies: active — galaxies: Seyferts — galaxies: starburst — infrared: galaxies — polarization

¹Institute of Geophysics and Planetary Physics, Lawrence Livermore National Laboratory, 7000 East Avenue, P.O. Box 808, L413, Livermore, CA 94550; htran@igpp.llnl.gov.

²National Optical Astronomy Observatories, P.O. Box 26732, Tucson, AZ 85726-6732.

³Department of Astronomy, University of California, Berkeley, CA 94720-3411.

⁴Department of Physics, University of California, Santa Barbara, CA 93106.

1. Introduction

Many sources in the *IRAS Faint Source Catalog (FSC)* exhibit enormous infrared luminosities ($L_{IR} > 10^{12} L_{\odot}$), and are known as ultraluminous infrared galaxies (ULIRGs, Sanders et al. 1988). These objects are an important constituent of our local Universe, with luminosities and space densities similar to those of quasi-stellar objects (Soifer et al. 1987). This led to the suggestion that ULIRGs could contain infant quasars enshrouded in a large amount of dust (Sanders et al. 1988). On the other hand, they may also represent energetic, compact starbursts (Condon et al. 1991). Understanding the dominant energy input mechanism in these ULIRGs – whether it is obscured quasars or intense bursts of star formation – has remained the main issue concerning their nature. Of particular interest are the “warm” ULIRGs (i.e., those having $f_{25}/f_{60} > 0.2$, Low et al. 1988; Sanders et al. 1988)⁵. They include a few of the exceptionally luminous sources, sometimes referred to as the “hyperluminous” ($L_{IR} \gtrsim 10^{13} L_{\odot}$) infrared galaxies, such as P09104+4109 ($z = 0.44$; Kleinmann et al. 1988), F15307+3252 ($z = 0.926$; Cutri et al. 1994), and F10214+4724 ($z = 2.286$; Rowan-Robinson et al. 1991). All of these galaxies have been shown to harbor a quasar nucleus obscured from direct view through the detection of hidden broad line regions (HBLRs) in polarized, scattered light (P09104+4109: Hines & Wills 1993; Tran 1998; F15307+3252: Hines et al. 1995; F10214+4724: Goodrich et al. 1996). This has led to the suggestion that perhaps all warm ULIRGs contain buried QSOs and that they may be the misdirected type 2 QSOs (AGN with Seyfert 2-like emission-line characteristics but QSO-like luminosities; Wills & Hines 1998).

With the exception of the above extreme *IRAS* sources, most of the known ULIRGs are relatively nearby ($z \lesssim 0.1$). In order to identify more ULIRGs at higher redshifts and study their population, several searches have been undertaken, using the positional correlation of sources in the *FSC* with those detected in deep radio surveys. Stanford et al. (1998) correlated objects in the *FSC* with those in the Faint Images of the Radio Sky at Twenty-cm (FIRST) catalog (Becker, White, & Helfand 1995), which has a flux density limit of ≈ 1 mJy. The results show that nearly all matches that are faint on the Palomar Observatory Sky Survey (POSS) turn out to be ULIRGs, if they lie on the well-known radio-to-far infrared (FIR) flux correlation (Condon et al. 1991) established by normal late-type galaxies and starburst galaxies at low redshifts. Spectroscopically, the vast majority of the sources ($\sim 85\%$) in this “radio-quiet” FIR sample (hereafter FF sources) can be classified as starburst systems (Stanford et al. 1998).

Dey & van Breugel (1994) correlated the Texas 365 MHz radio catalog (Douglas et al. 1996) with an early version of the *FSC*, and selected from this sample those sources that lie *above* the radio-to-FIR flux-flux correlation (see Sopp & Alexander 1991; Colina & Pérez-Olea 1995; Stanford et al. 1998). From this sample (hereafter TF sources) they discovered a significant class of gas and dust-rich AGN which are characterized by large FIR luminosities, and which are intermediate in

⁵ f_{25} and f_{60} are the *IRAS* flux densities in units of Jy at 12 μm and 60 μm , respectively.

radio luminosity, FIR color, and optical spectral class between the *IRAS* ultraluminous galaxies and powerful quasars (Dey & van Breugel 1994; Stanford et al. 1998). Because of the much higher detection threshold of the Texas survey (≈ 150 mJy, Douglas et al. 1996), the majority of these sources are “radio-loud” LINERs, Seyfert 2s and post–starburst active galactic nuclei (PSAGN). The latter are characterized by the strong Balmer absorption lines, Seyfert 2-like emission lines and compact, often almost stellar, optical morphologies.

A notable feature of both the radio-quiet and radio-loud FIR starburst and PSAGN objects, visible in high signal-to-noise spectra, is the prevalence of many strong high- n Balmer absorption lines ($EW \sim 10 \text{ \AA}$), as well as a strong Balmer discontinuity in their spectra. These features signify a large population of hot, relatively young stars ($10^8 - 10^9$ yrs). In addition, their emission-line spectra tend to exhibit a very low ionization state, as characterized by the strength of [O II] $\lambda 3727$ relative to [O III] $\lambda 5007$ ([O II] $\lambda 3727$ /[O III] $\lambda 5007 \gtrsim 2$), and the lack or weakness of high-ionization lines such as [Ne V] $\lambda 3426$. Qualitatively, the spectra of these galaxies appear very similar to those of the class of galaxies called “E + A” or “post-starburst” galaxies (Dressler & Gunn 1983; Oegerle, Hill, & Hoessel 1991; Wirth, Koo, & Kron 1994; Liu & Green 1996), whose spectra display not only the 4000 \AA break, G-band, and MgI b features that are indicative of an old (~ 10 Gyr) stellar population (the “E” component), but also the Balmer absorption lines characteristic of much younger stars (< 1 Gyr, the “A” component). Many FF and TF sources appear to differ from E + A galaxies only in the additional presence of emission lines, indicating the presence of on-going star formation or active galactic nuclei (see spectra of TF J1020+6436 and FF J1614+3234 below). These objects may form an important evolutionary link between starbursts and quasar activity (Canalizo & Stockton 1997; Stockton, Canalizo, & Close 1998).

In order to better understand the energy sources of ULIRGs and the relationship between AGN and starburst activity, we started a spectropolarimetric survey to search for hidden broad emission lines in both types of objects: the radio-quiet (FF) and radio-loud (TF) ULIRGs. This would indicate whether obscured AGNs might exist, and the high signal-to-noise data might be used to investigate the nature of their stellar populations. This might be used to help quantify the relative importance of quasar and starburst activity, and to search for possible correlations with the age of the starbursts, luminosity, and morphological evolution.

This paper reports the first results for three objects with $L_{IR} \gtrsim 10^{12} L_{\odot}$ ⁶: TF J1020+6436, TF J1736+1122, and FF J1614+3234. Only TF J1736+1122 is certainly IR “warm” with $f_{25}/f_{60} = 0.404$. For TF J1020+6436 and FF J1614+3234, only an upper limit of the f_{25} flux density was obtained. Table 1 lists the infrared properties for the three objects. Throughout this paper, we assume $H_o = 75 \text{ km s}^{-1} \text{ Mpc}^{-1}$, $q_o = 0$ and $\Lambda = 0$.

⁶ L_{IR} is calculated by following the prescription of Sanders & Mirabel (1996).

2. Observations and Reductions

2.1. Spectropolarimetry

Spectropolarimetric observations were made with the polarimeter (Cohen et al. 1997) installed in the Low Resolution Imaging Spectrometer (LRIS, Oke et al. 1995) on the 10-m Keck II telescope on the night of 1997 April 10 (UT). A $1''$ wide, long slit oriented at the parallactic angle was centered on the nucleus of each galaxy. We used a $300 \text{ grooves mm}^{-1}$ grating which provided a dispersion of $2.46 \text{ \AA pixel}^{-1}$ and a resolution of $\sim 10 \text{ \AA}$ (FWHM). The observations were made by following standard procedures of rotating the half waveplate to four position angles (0° , 22.5° , 45° , and 67.5°), and dividing the exposure times equally among them. The total exposure times were one hour each for TF J1020+6436 and FF J1614+3234, and 40 minutes for TF J1736+1122. We followed standard polarimetric reduction techniques as described, for example, by Cohen et al. (1997).

2.2. Near-Infrared Imaging

Near-IR observations of FF 1614+3234 were made using the Near Infrared Camera (NIRC, Matthews & Soifer 1994) at the Keck I Telescope. NIRC employs a 256×256 InSb array with a scale of $0.15 \text{ arcsec pixel}^{-1}$. The data were obtained through a K_s filter on 1998 April 18 (UT), under photometric conditions with $\sim 0''.5$ seeing. The target exposures were taken using a nonredundant dithering pattern, with individual shifts between pointings of $3''$. Integration times for each pointing were typically 60 s comprised of 3 coadds; the total on-source exposure time was 1920 s. After bias subtraction, linearization, and flatfielding (using sky flats), the data were sky-subtracted, registered and summed using the DIMSUM⁷ near-IR data reduction package. Subsequent photometry was flux calibrated via short observations of UKIRT faint standards (Casali & Hawarden 1992), which, after a suitable transformation, yields magnitudes on the CIT system.

Figure 1 shows the K_s -band image of FF J1614+3234 obtained with Keck I Telescope. As can be seen, the near-IR image shows a disturbed morphology, with an extension separated $\sim 1''.8$ from the nucleus to the south-west. At a lower surface brightness level, extended filamentary arc-like structure is present to the north and west. This feature is suggestive of a tidal tail due to a merger event or interaction. There is also an apparent companion $\sim 2''.2$ to the north-west. These features are consistent with FF J1614+3234 being similar to an E + A galaxy, which often occurs in merging systems (e.g., Liu & Kennicutt 1995). They also provide strong circumstantial evidence that any starburst and AGN activity present is triggered by galaxy interaction. No

⁷DIMSUM is the Deep Infrared Mosaicing Software package, developed by P. Eisenhardt, M. Dickinson, A. Stanford, and J. Ward, and is available as a contributed package in IRAF.

indication of gravitational lensing is evident from the image.

2.3. Radio Observations

TF J1020+6436 and TF J1736+1122 were both observed with the VLA, using standard bandwidths and calibrations, to obtain more accurate positions, and morphological and spectral index information. TF J1020+6436 was observed at 4860 MHz in the C-array and was found to be unresolved with an angular size $< 1''$. TF J1736+1122 was observed at 4860 MHz and 8440 MHz in the B and A-arrays respectively. The B-array observations showed that this source was slightly resolved, with an angular size of $0''.9 \times 0''.4$, at $PA = 89^\circ$. In the A-array, and at the higher frequency of 8440 MHz, the source shows a resolved core with a clear double structure (see Fig. 2) elongated along $PA \sim 97^\circ$. This structure axis is essentially perpendicular ($\Delta PA \approx 80^\circ$) to the polarization PA of 18° (see §4.1), as has been found for many polarized narrow-line radio galaxies and Seyfert 2 galaxies (e.g., Tran et al. 1998 and references therein). For FF J1614+3234 the radio data was taken from the FIRST catalog (Becker et al. 1995). Only the 1400 MHz observations are available for this source, which is unresolved with an angular size of $< 4''$. The positions and flux densities of the three sources are listed in Table 2.

It is of interest to note that the radio continua of the two radio-loud TF sources have quite steep spectra, with spectral indices $\alpha \sim -1$ ($f_\nu \propto \nu^\alpha$). In the case of TF J1736+1122 the radio spectrum steepens significantly between 365 MHz and 8440 MHz, with α changing from -0.75 to -1.45 (see Table 2). In addition, both objects are quite small (< 2.6 kpc). Such compact steep spectrum (CSS) radio sources comprise a significant fraction of complete radio source surveys, and are thought to be “frustrated” or young radio sources whose jets are plowing through the dense ISM of their parent galaxies (see O’Dea 1998 for a recent discussion).

3. Results

3.1. Line Ratios, Diagnostics, and Classification

Table 3 presents the integrated emission-line flux ratios and their rest-wavelength equivalent widths. The emission-line fluxes were measured from the starlight-subtracted spectra. For FF J1614+3234 and TF J1020+6436, isochrone population synthesis models of the underlying young starbursts (see §3.2) have been removed. For TF J1736+1122, the contribution from an old stellar population represented by the elliptical galaxy NGC 4478 was used (§3.3). In TF J1736+1122, the narrow emission lines display extended wings that cannot be adequately fit with a single Gaussian profile. A sum of two Gaussian profiles, one with $FWHM \sim 500 \text{ km s}^{-1}$ and another with $FWHM \sim 1300 - 1800 \text{ km s}^{-1}$ but identical center, is able to reproduce the observed profiles very well. The observed spectrum of TF J1020+6436 appears to suffer significant internal

reddening. The measured narrow-line Balmer decrement is $H\alpha/H\beta = 8.8$, giving an extinction of $E(B - V) = 1.05$, assuming an intrinsic ratio of $H\alpha/H\beta = 3.1$ and using the extinction law of Cardelli, Clayton, & Mathis (1989).

Plotting the line flux ratios (involving [O II] $\lambda 3727$, $H\beta$, [O III] $\lambda 5007$, [N II] $\lambda\lambda 6548, 6583$, $H\alpha$, [S II] $\lambda 6724$, and [O I] $\lambda 6300$) on the diagnostics diagrams of Baldwin, Phillips, & Terlevich (1981) and Veilleux & Osterbrock (1987) shows that both TF J1020+6436 and TF J1736+1122 lie in regions typically occupied by narrow-line AGNs. This suggests that the dominant energy input in the narrow line regions (NLRs) is photoionization by a hard continuum. These objects can be classified as Seyfert 2 galaxies. However, only TF J1736+1122 can be called a *bona fide* high-ionization Seyfert 2. Although TF J1020+6436 formally qualifies as a type 2 Seyfert, its ionization level is quite low ($[O II] \lambda 3727/[O III] \lambda 5007 = 1.4$). What clearly separates it from TF J1736+1122 is the domination of early-type stellar spectral features in the blue end of the spectra. TF J1020+6436 satisfies half of the definition of Heckman (1980) for LINERs⁸: $[O II]/[O III] > 1$. The other half of the criterion is not satisfied ($[O I]/[O III] = 0.15 < 0.33$, Table 3), and thus it is not a LINER, and we adopt the Seyfert 2 classification for it. Since our spectrum of FF J1614+3234 does not cover wavelengths longward of [O III] $\lambda 5007$, an unambiguous classification of this galaxy based on the line ratios of [N II], $H\alpha$, and [S II] is not possible. Using the available line strengths, we classify FF J1614+3234 as a LINER based on the low ionization level ($[O II] \lambda 3727/[O III] \lambda 5007 = 1.75$; $[O III] \lambda 5007/H\beta = 2.0$) and the strong appearance of hot-star spectral features.

3.2. No Detection of Hidden Quasars in FF J1614+3234 and TF J1020+6436

FF J1614+3234 and TF J1020+6436, whose total flux spectra and Q and U Stokes parameters are shown in Figure 3, display no significant detectable polarizations. A formal averaging of the continuum polarization over the observed wavelength range $4500 \text{ \AA} - 8000 \text{ \AA}$ gives $P = 0.24\% \pm 0.18\%$ and $0.15\% \pm 0.15\%$ (uncorrected for biasing) in FF J1614+3234 and TF J1020+6436, respectively. As a result, we detected no polarized broad lines in the spectra of two of the more luminous ULIRGs in our sample. There is also little sign of Mg II $\lambda 2800$ in the spectrum of FF J1614+3234. It shows a very weak feature at the wavelength expected for Mg II $\lambda 2800$, but the profile is highly irregular. Although the non-detection of hidden broad lines, by itself, does not rule out the presence of a quasar, as the geometry may not be propitious for scattered light to reach our line of sight (e.g., blockage or lack of scattering region, high viewing inclination), the low excitation state and the presence of strong Balmer absorption lines seem to indicate that the energy output is dominated by a young starburst. The enormous IR luminosity is likely the result of this starburst activity.

⁸Criteria for LINERs as defined by Heckman (1980) are: $[O II] \lambda 3727/[O III] \lambda 5007 > 1$ and $[O I] \lambda 6300/[O III] \lambda 5007 > 1/3$.

We used the GISSEL models of Bruzual & Charlot (1996, BC96) to characterize the young stellar population dominating the spectra of FF J1614+3234 and TF J1020+6436. We assumed an instantaneous burst of star formation with a Salpeter (1955) initial mass function having a mass range $0.1M_{\odot} < M < 125M_{\odot}$ and solar metallicity. The fit is a χ^2 minimization of the sum of a blue featureless continuum (representing the Seyfert 2/LINER ionizing continuum) and the young starburst model. Our analysis indicates that some additional reddening is also required for a good fit. Using the starburst extinction curve of Calzetti, Kinney, & Storchi-Bergmann (1994), the required reddening is $E(B - V) \sim 0.3$ for FF J1614+3234 and ~ 0.35 for TF J1020+6436. Figure 4 shows the best fits to the observed spectra, which were achieved for a starburst with an age of 320 Myr. This is consistent with the median age derived for the starburst knots found in all of the ULIRGs studied by Surace et al. (1998) using *HST* imaging. Our results show that the light from the 320 Myr-old starburst component contributes about 68% and 76% of the total light at 4200 Å (rest frame) for FF J1614+3234 and TF J1020+6436, respectively. The rest of the light is due to the blue ionizing continuum of the Seyfert 2/LINER nucleus and perhaps an even younger population of hot (OB) stars.

3.3. TF J1736+1122: Hidden Broad Lines and Starburst Activity

Unlike the two ULIRGs discussed above, TF J1736+1122 is highly polarized, having a continuum P reaching up to $\sim 23\%$ in the near-UV. The spectropolarimetry is shown in Figure 5. The polarized flux spectrum, $P \times F_{\lambda}$, clearly displays not only broad Balmer emission lines of $H\alpha$, $H\beta$, $H\gamma$, but also the Fe II blends near 4570 Å and 5250 Å. In this respect, it is similar to the $P \times F_{\lambda}$ spectrum of the hidden Seyfert 1 galaxy NGC 1068 (Miller, Goodrich & Mathews 1991; Tran 1995).

We corrected the polarization for a small amount of interstellar polarization (ISpol), based on the polarization of the narrow [O II] emission line and the polarization of several stars near the line of sight to TF J1736+1122. The ISpol we adopt is $P = 0.4\%$ at $PA = 80^{\circ}$. This is consistent with the maximum polarization expected ($P_{max} < 9.0E(B - V)$; Serkowski, Mathewson, & Ford 1975) from the Galactic reddening toward TF J1736+1122 ($E(B - V) = 0.144$; Burstein & Heiles 1984). Since the correction is small relative to the polarization of TF J1736+1122, it does not significantly affect the results or alter our conclusions.

We also corrected the observed polarization for the unpolarized starlight in the host galaxy (e.g., Tran 1995). Unlike FF J1614+3234 or TF J1020+6436, the underlying stellar population of TF J1736+1122 is dominated by old ($>$ a few Gyr) stars, as indicated by the lack of Balmer absorption lines. Accordingly, a selection of normal elliptical galaxies was tried in the fit, and the best fitting template galaxy is NGC 4478. We derived a galaxy fraction of 0.52 at 5500 Å. Before starlight subtraction the percentage of polarization rises rapidly with shorter wavelength, reaching $\sim 23\%$ at 3250 Å. This rise in P is due to the decreasing dilution of starlight at shorter wavelengths, as the starlight-corrected polarization is essentially flat. There is a rise in polarization

in the broad wings of $H\alpha$ and $H\beta$, signifying the presence of a second diluting “featureless continuum” (FC2), perhaps due to hot stars (Cid Fernandes & Terlevich 1995; Heckman et al. 1997) or thermal radiation from hot electrons (Tran 1995).

The presence of hot stars, perhaps arising in a starburst, is suggested by the broad feature underlying He II $\lambda 4686$. This broad feature is shown in Figure 6 as a residual after the narrow line components are fitted and subtracted. This feature cannot be a broad scattered He II component since it appears very strongly in the total flux spectrum, suggesting that the light is viewed directly, and it is not detected in the $P \times F_\lambda$ spectrum (Fig. 5). It can be attributed to Wolf-Rayet (W-R) stars, as has been identified by Heckman et al. (1997) in Mrk 477 and Storchi-Bergmann, Cid Fernandes, & Schmitt (1998) in Mrk 1210, both of which are Seyfert 2 galaxies with hidden broad-line regions, and for which a large fraction of FC2 has been inferred (Tran 1995). It seems, therefore, that there is a large number of young and/or W-R stars in TF J1736+1122, which contributes to the observed FC2. As discussed by Schaerer & Vacca (1998), the presence of this feature indicates that the time elapsed since the last burst of star formation cannot be more than a few Myr. If we assume that the broad feature is all due to the “W-R bump” and that $H\beta$ emission arises entirely from massive stellar activity (clearly an overestimate since most of the $H\beta$ must be due to the AGN), we can derive an absolute lower limit to the ratio of W-R to O stars. Using the relation derived by Schaerer & Vacca (1998) (their Fig. 22 and equ. 17), the observed W-R bump/ $H\beta$ ratio of 0.14 (Table 3) gives a W-R/O star number ratio > 0.2 . By contrast, there is little sign of the W-R bump in either FF J1614+3234 or TF J1020+6436, suggesting that the number of W-R stars relative to O stars must be low. This may indicate that few of the most massive stars ($\gtrsim 35 M_\odot$, which turn into W-R stars) are formed in these galaxies, or their star formation episodes, which may still be ongoing, last longer than in TF J1736+1122.

4. Discussion

4.1. Modelling of the Continuum and Line Polarization in TF J1736+1122

In order to separate the line and continuum components of polarization of TF J1736+1122, we modelled the observed spectropolarimetric observations. Following a method similar to that described by Tran et al. (1997), we model the spectropolarimetry surrounding the $H\alpha + [\text{N II}]$ complex by simultaneously fitting the continuum and emission-line components in the total flux, $Q \times F_\lambda$, and $U \times F_\lambda$ spectra. The broad $H\alpha$ in $P \times F_\lambda$ is best fitted by two Gaussian profiles with FWHMs of 18000 km s^{-1} and 4900 km s^{-1} , giving a combined FWHM of 5580 km s^{-1} . We use this same 2-component model to fit the $H\alpha$ line profile in the total flux spectrum. The narrow lines of $H\alpha + [\text{N II}]$, $[\text{O I}]$, $[\text{S II}]$ were fitted assuming that they are similarly polarized, and having Gaussian profiles with FWHMs similar to that of the $[\text{O III}]$ lines ($\sim 840 \text{ km s}^{-1}$). The results of our polarization modelling are shown in Figure 7.

The results indicate that the broad-line polarization is very high, $\sim 50\%$, while the continuum

P is much lower at $\sim 22\%$, both at a similar PA of 20° . This indicates that the amount of unpolarized FC2 flux relative to the total continuum (i.e., FC1 + FC2) would be about 60% in order to make the continuum and broad-line polarizations equal. This is also just the amount required in order to scale up the polarized flux spectrum and subtract off the broad-line component from the total flux spectrum. Our fitting also shows that the narrow lines possess a small amount of polarization $\sim 0.4\%$ at PA = 162° . They are clearly polarized at a PA different from that of the broad line and continuum, as evidenced by the apparent absorption in the $P \times F_\lambda$ spectrum at the wavelengths of strong narrow emission lines such as [O III] $\lambda\lambda 4959, 5007$ (Fig. 5). The results found here are similar to all prior results for Seyfert 2 and narrow line radio galaxies, (e.g., Tran 1995; Tran, Cohen, & Goodrich 1995; Cimatti et al. 1996; Dey et al. 1996; Tran et al. 1998) in that they all show the presence of an FC2, an old stellar population, high polarization in the continuum and broad lines but little or no polarization in the narrow lines.

Polarization modelling at $H\beta + [\text{O III}]$ shows similar results for the broad-line and continuum polarization. However, the fitting here is complicated by the presence of strong underlying optical Fe II emission, and thus the results are not as well constrained. However, the similar polarizations obtained suggest that the polarization is independent of wavelength.

The continuum polarization PA shows a slight rotation of $\sim 4^\circ$ from 16° to 20° across the wavelength range covered. This may mean that FC2 is slightly polarized or that there is some small interstellar polarization internal to the host galaxy. Any of these effects is expected to be small since there is little or no difference in the polarization PA between the continuum and broad lines at $H\alpha$ or $H\beta$.

4.2. Polarized Flux Spectrum and Fe II emission in TF J1736+1122

The luminosity of the hidden broad-line AGN indicates that it is consistent with being a quasar. Using the formulation of Véron-Cetty & Véron (1996), the observed absolute magnitude of TF J1736+1122 is $M_B \approx -21.2$. Assuming an optically thin, uniformly filled scattering cone with half-opening angle of 40° oriented at an inclination of 70° (§4.4), producing an intrinsic polarization of 50%, we derive $f_{\text{direct}}/f_{\text{scattered}} \approx 10$ (see e.g., Brotherton et al. 1998). Thus the luminosity of the obscured source is $M_B \approx -23.7$, marginally qualifying its status as a quasar. With an optical spectral index of $\alpha \sim -0.24$ ($f_\nu \propto \nu^\alpha$), the scattered ($P \times F_\lambda$) spectrum of TF J1736+1122 also appears very similar to the composite quasar spectrum of Francis et al. (1991), which has $\alpha = -0.32$. The Balmer decrement in $P \times F_\lambda$ is 4.2 ± 1 . These results indicate that there is no significant “bluening” or reddening of the scattered spectrum. Thus it appears that the scatterer is gray, as would be the case for electrons. For comparison, the Balmer decrement in the NLR is $H\alpha/H\beta = 2.9$, also essentially unreddened by dust.

As has been mentioned, an interesting feature in the $P \times F_\lambda$ spectrum of TF J1736+1122 is the presence of strong polarized Fe II emission. The rest-frame EWs of the Fe II blends at

4570 Å and 5250 Å are ≈ 35 Å and 50 Å, respectively⁹. This is comparable to those seen in normal quasars, Seyfert 1, and broad-line radio galaxies (e.g., Joly 1991). The detection of Fe II in $P \times F_\lambda$ is rather surprisingly rare among the class of polarized broad-line AGNs. Of all the Seyfert 2s and narrow-line radio galaxies known to show HBLRs (Tran 1995; Tran et al. 1995; Young et al. 1996; Cohen et al. 1998) only NGC 1068 and Mrk 463E have been observed previously to show optical Fe II in their $P \times F_\lambda$ spectra.

Although optical Fe II emission in AGNs has been known for many years, its exact nature and origin are still not fully understood. The strength of Fe II emission tends to be weaker in broad-line radio galaxies compared to radio-quiet Seyfert 1 galaxies (e.g., Osterbrock 1977). This general tendency between Fe II strength and radio-loudness also holds for QSO and quasars (Boroson & Green 1992), but radio-loud objects are by no means always weak Fe II emitters (e.g., Joly 1991). Among the radio-loud quasars, it has been found (e.g., Heckman 1983; Jackson & Browne 1991; Brotherton 1996) that Fe II strength is correlated with radio spectral index, in the sense that flatter-spectrum sources display stronger optical Fe II. TF J1736+1122 has a radio spectrum that is rather steep (Table 2). Its radio-to-optical flux ratio and radio luminosity (Table 2) indicate that TF J1736+1122 is formally radio-loud, albeit only marginally. In the orientation-dependent model of quasars, flat-spectrum radio sources are thought to be those viewed at small inclination angle where the core component dominates, while steep-spectrum radio sources are those viewed at larger viewing angle where the lobes dominate (e.g., Orr & Browne 1982; Boroson & Oke 1984). Thus, TF J1736+1122 could be a radio-loud quasar being viewed at large inclination angle, with heavy obscuration by dust, perhaps in the form of a putative torus, dominating the central nucleus.

Because Fe II emission appears prominently in broad-line (type 1) AGNs, in which the nuclear and BLR radiation escape freely in our direction, it is thought to be associated closely with the ionizing continuum, BLR and radio core (e.g., Zheng & Keel 1991). However, several observations (Hickson & Hutchings 1987; Canalizo & Stockton 1997) have shown that Fe II emission in the QSO PG 1700+518 varies spatially, suggesting that it could come from more extended regions, perhaps in a superwind and shocks generated by supernovae and supernova remnants of a starburst (Terlevich et al. 1992). Since the polarization magnitude and position angle of the continuum, broad emission lines, and Fe II emission are virtually identical in TF J1736+1122, indicating that they must all follow the same scattering geometry, our results support the picture in which Fe II emission originates from a compact source very close to the nucleus, arguing against an extended supernova origin for Fe II.

⁹The Fe II EWs were measured by scaling and broadening the Fe II template I Zw 1 to fit the observed blends, as described by Boroson & Green (1992).

4.3. Detection of HBLRs and Nature of ULIRGs: Starburst versus AGN

The original motivation for the HBLR search of ULIRGs in the present study was initiated by their positions in the radio-FIR correlation diagram. Based solely on their general coincidence with the hyperluminous *IRAS* galaxies in this diagram, and Sanders et al. (1988) ULIRG-quasar evolutionary scheme, we would expect them to harbor obscured quasars. This expectation has not been borne out. The lack of polarization in TF J1020+6436 and FF J1614+3234 raises an important question: if a BLR is not detected in polarized light, does it truly not exist? While we cannot rule out the presence of an obscured quasar in these sources, it appears that if a quasar BLR exists, its presence ought to betray itself by some tell-tale signs. With sufficiently high signal-to-noise ratio (S/N), a BLR should be readily observed if it is present. It could be that the polarized signal is swamped by unpolarized light and is undetectable, or perhaps other factors such as the geometry and distribution of the surrounding medium are less than optimal for scattered light to reach our line of sight. In such cases, little or no light from the central BLR could be observed even if it existed. There are reasons to suggest that although this situation may well be possible, it is unlikely. First, if the quasar “monster” is present, deep, high S/N observation at Keck should be able to reveal it, even in the presence of a relatively large starlight fraction. This has been demonstrated by the spectacular detection of broad Balmer lines in Cygnus A (Ogle et al. 1997), which have long been sought after in previous fruitless attempts (Goodrich & Miller 1989; Jackson & Tadhunter 1993). At the level of S/N of the present observations, we should have easily detected the broad lines if they were present at a polarized flux level similar to that in Cygnus A. Second, a detection of broad polarized emission lines in an object dominated by a strong Balmer absorption-line (A star) spectrum would be unprecedented. Of the approximately two dozen HBLR type 2 AGNs detected by spectropolarimetry to date (e.g., Tran 1995; Tran et al. 1995; Young et al. 1996; Tran et al. 1998; Cohen et al. 1998), *none* fits this description. The most likely, and reasonable explanation for this is that such objects do not exist or are very rare. The similar galaxy fractions detected in systems both with and without strong Balmer absorption lines (§3.2, 3.3) make it unlikely that the lack of detectable polarization (and hence of hidden quasar) in the former is simply due to the large dilution of scattered light by hot stars. If we believe in a scenario in which both the QSO and starburst activities are triggered by close interaction and can coexist (Stockton 1998), then this may imply that the life times of the “starburst phase” of QSOs are very short, comparable to those of the most massive stars. Third, our finding is consistent with the conclusions reached by the near-infrared spectroscopic study of Veilleux et al. (1997), who showed that the optically LINER-like ULIRGs do not show any evidence for broad Paschen lines or strong high-ionization [Si VI] emission (which would signify the presence of a genuine monster). By contrast, most, if not all (7–9 out of 10) of the Seyfert 2 ULIRGs in their sample were found to display obscured BLR and strong [Si VI]. Since TF J1020+6436, and perhaps FF J1614+3234 are marginal Seyfert 2s, borderlining LINERs, they are not expected to contain hidden BLRs.

Since the ULIRG phenomenon appears to be a mix of either AGN-dominated and starburst-dominated events, it is of interest to see if it could be determined, from optical spectroscopic and

IRAS photometric data alone, whether an ULIRG harbors a genuine quasar or is powered by a starburst. The above results suggest that the emission-line ionization level of an ULIRG plays an important role in identifying the main power source. Another important factor is the IR color f_{25}/f_{60} , as it has been shown that the success of detecting HBLRs is well correlated with this ratio in both Seyfert 2 galaxies (Heisler, Lumnsden, & Bailey 1997) and ULIRGs (Veilleux et al. 1997). Figure 8 shows a plot of the line ratio $[\text{O III}] \lambda 5007/\text{H}\beta(\text{narrow})$, which can serve as an indicator of the ionization level, versus f_{25}/f_{60} . Shown are those narrow-line ULIRGs in which HBLRs have been actively searched for either in near-IR spectroscopy (Veilleux et al. 1997), or optical spectropolarimetry (this paper). They include not only Seyfert 2 galaxies, but also sources classified as H II and LINERs with available line ratios and IR colors. Most optical spectroscopic data are obtained from Veilleux et al. (1995) and Kim, Veilleux, & Sanders (1998). We also include a few other well-known ULIRGs (Arp 220, Mrk 273, NGC 6240, UGC 5101), the three “hyperluminous” sources (F10214+4724, P09104+4109, F15307+3252), as well as Mrk 463E, a Seyfert 2 galaxy harboring HBLR with $L_{IR} = 10^{11.8} L_{\odot}$. As can be seen, there is a clear tendency for higher-ionization and “warmer” Seyfert 2 ULIRGs to show HBLR indicative of a “buried quasar.” Furthermore, Seyfert ULIRGs without HBLRs lie in a region of the diagram similar to that occupied by H II and LINER galaxies, none of which has been found to have HBLRs.

Figure 8 is analogous to the diagnostic diagram of Genzel et al. (1998), who use a plot of the mid-IR line ratio $[\text{O IV}] 25.9 \mu\text{m}/[\text{Ne II}] 12.8 \mu\text{m}$ versus the strength of the $7.7 \mu\text{m}$ PAH (polycyclic aromatic hydrocarbons) feature, and to that of Lutz et al. (1998), who use the same PAH feature and the $5.9\mu\text{m}/60\mu\text{m}$ continuum flux ratio, to separate out ULIRGs that are predominantly powered by AGN or starburst. Unlike these diagrams, however, Figure 8 not only involves the much more accessible (for moderate redshifts) optical lines of $[\text{O III}]$ and $\text{H}\beta$, but can also identify those AGNs harboring hidden quasars.

Thus, it appears that when an IR-luminous object displays a very high IR luminosity (ultraluminous), is relatively “warm”, and shows a high-ionization spectrum characteristic of Seyfert 2 galaxies, it would most certainly contain an HBLR, (i.e., it is truly a buried quasar). TF J1736+1122, for example, shows a classic strong-ionization Seyfert 2 spectrum, a warm f_{25}/f_{60} color of 0.404, an IR luminosity of $L_{IR} \approx 10^{12} L_{\odot}$, and is observed to show a spectacular HBLR. It is highly polarized, with properties that are consistent with there being a quasar. FF J1614+3234, on the other hand, has an extremely high $L_{IR} (> 10^{12.6} L_{\odot})$, placing it in the company of the hyperluminous IR galaxies, and may be relatively warm ($f_{25}/f_{60} < 0.31$), but displays a feeble LINER spectrum. It is not polarized and there is no evidence of any hidden broad lines. The one characteristic that the ULIRGs with HBLR have in common is the display of classic high-ionization optical spectrum of a Seyfert 2. This then appears to be a necessary condition for an ULIRG to harbor a buried quasar.

4.4. The Influence of Quasars on Diagnostic Properties of ULIRGs

We now discuss how these three conditions – ionization level, IR luminosity, and IR color – are related to the existence of an obscured quasar in these AGNs.

a) High-ionization Seyfert 2 spectrum: This is necessary because a hard power-law input spectrum is needed to produce the high-ionization emission lines characteristic of an AGN. This is most likely produced by an accretion disk feeding a central black hole rather than by a population of hot stars, or bursts of star formation (with possible additional contributions from shocks).

b) High IR luminosity: Veilleux et al. (1995) and Kim et al. (1998) have found that the fraction of Seyfert galaxies among luminous infrared galaxies increases dramatically for $L_{IR} > 10^{12} L_{\odot}$. It follows naturally then that the number of galaxies with HBLRs also increases with IR luminosity. The enormous L_{IR} in these objects likely arises from reprocessed optical/UV/X-ray radiation of the ionizing continuum which was absorbed by the putative dusty molecular torus surrounding the central engine (e.g., Granato, Danese, & Franceschini 1996).

c) Warm IR color: Hutchings & Neff (1991) and Kay (1994) have suggested that HBLR Seyfert galaxies tend to show warmer IR color. This has recently been confirmed by Heisler et al. (1997) in their survey of southern Seyfert 2 galaxies. They suggest that this trend could be explained in the context of the obscuring torus paradigm, where Seyfert 2s with HBLRs are those viewed at intermediate but not too high an inclination angle, so that our line of sight encompasses much of the inner, warmer regions of the dusty torus. Since the dusty torus could be optically thick even to mid-IR photons ($12\mu\text{m}$ – $25\mu\text{m}$, Dopita et al. 1998), at larger viewing angle, our line of sight intercepts mostly the outer, cooler gas and dust in the torus, giving rise to a Seyfert 2 with cool IR color and no detectable HBLR. This implies that the scattering takes place very close to the central region. The same picture may also be true in the ULIRGs, leading to a similar correlation between the visibility of HBLR and warmth (Veilleux et al. 1997; Fig. 8).

The viewing inclination to these objects can in principle be constrained by the inferred intrinsic polarization of these ULIRGs, and thus provides a way to test the above interpretation. The polarizations from ULIRGs with HBLRs are generally very high (~ 20 – 30%), indicating that the viewing angle is also large. The highest intrinsic polarization observed is perhaps that of TF J1736+1122 presented in this paper with $P \sim 50\%$. For a uniformly filled cone of optically thin scattering material with a typical half-opening angle of $\sim 40^\circ$ (e.g., Wilson & Tsvetanov 1994), we obtain an inclination angle of $i \sim 70^\circ$, based on the model of Brown & McLean (1977) (see also Miller & Goodrich 1990; Miller et al. 1991; Wills et al. 1992; Balsara & Krolik 1993; Hines & Wills 1993; Brotherton et al. 1998). This seems too high for the picture proposed by Heisler et al. If multiple scattering in clumpy clouds as well as dichroic extinction by optically thick gas contribute, the intrinsic polarization would be lower (Kartje 1995; Kishimoto 1996), and thus i would have to be even higher. Similarly, if the cone opening angle is larger than 40° , the inferred i would be higher for a given P . For smaller cone or torus opening angle, the required i would be reduced, but the fraction of scattered light intercepted by the observer would also be much

less. For example, if the half-opening angle were 20° , i would be $\approx 58^\circ$, but the fraction of light scattered would be reduced by a factor of 3.5, making it much harder to detect the polarization. In any case, for $P = 50\%$, i cannot be smaller than $\sim 55^\circ$, at which point virtually no light gets scattered from the hidden quasar since the cone would be infinitely narrow. Thus it seems likely that our viewing angle to TF J1736+1122 is $\gtrsim 70^\circ$, and yet broad polarized emission lines are easily seen and a warm IR color is detected, in contrast to the expectations of the Heisler et al. interpretation.

An alternative picture is that, in the case of the ULIRGs, the warmth of the source, as well as the high-ionization level, is a direct result of the very presence of a quasar “monster” in the nucleus, and not solely a consequence of our viewing angle. Apparently, in order for dust grains to radiate efficiently at $25 \mu\text{m}$, heating sources with very high energy densities (e.g., AGN) may be required (cf., Rowan-Robinson & Crawford 1989; Condon, Anderson, & Broderick 1995). In most “cold” ULIRGs the quasar simply does not exist, has not yet had sufficient time to form, or has burned out; the energetics are instead dominated by starburst, H II region, or LINER activity. The lack of HBLRs in these types of objects is unlikely to be due to dust obscuration (e.g., Veilleux et al. 1997), since even in such cases scattered broad lines could still be observed.

5. Conclusions

Although evidence of starburst activity is found in all three objects of the present study, some ULIRGs are powered predominantly by quasars, and some are mainly energized by starbursts with no indication of an obscured AGN. Thus their high IR luminosity of $\sim 10^{12}\text{--}10^{13} L_\odot$ does not guarantee the presence of a quasar in the center of these objects, such as those found in other well-known ULIRGs (e.g., F10214+4724, P09104+4109, and F15307+3252). Apparently, there is a class of galaxies which have IR luminosities similar to those of the “classical” *IRAS*-warm galaxies but there are no detectable quasars residing in them. The ULIRG phenomenon, therefore, can be both explained by the presence of a quasar or a powerful starburst.

We discovered a new hidden broad-line *IRAS* galaxy TF J1736+1122, which is intrinsically highly polarized ($\sim 50\%$ in broad $\text{H}\alpha$), independent of wavelength. The obscured source has characteristics consistent with it being a quasar. The detection of HBLR in this galaxy and the non-detections in FF J1614+3234 and TF J1020+6436 are consistent with the idea that buried quasars preferentially reside in ULIRGs having warm colors, but with the necessary condition that their spectra must show characteristics of a high-ionization Seyfert 2 galaxy. Quasar-hosting galaxies also seem to have a preference for a *dominant* stellar population that is old (> 1 Gyr), while galaxies without detectable sign of a quasar display a younger stellar population. If the AGN and starburst activities in these objects are triggered by the same mechanism at the same time (cf. Stockton 1998), then our findings indicate that quasars are likely to be found only in evolved systems with age $\gtrsim 300$ Myr. More observations of a larger sample of ULIRGs, and especially of quasar host galaxies are needed to further examine this issue.

We thank Carlos “the mad Belgian” De Breuck for fruitful discussions, and Jan Tweed for her assistance with Figure 2. The W. M. Keck Observatory is operated as a scientific partnership between the California Institute of Technology and the University of California, made possible by the generous financial support of the W. M. Keck Foundation. Work performed at the Lawrence Livermore National Laboratory is supported by the DOE under contract W7405-ENG-48. R.A. acknowledges the support of NSF grant AST-9617160. This research has made use of the NASA/IPAC Extragalactic Database (NED) which is operated by the Jet Propulsion Laboratory, California Institute of Technology, under contract with the National Aeronautics and Space Administration.

REFERENCES

- Balsara, D. S., & Krolik, J. H. 1993, *ApJ*, 402, 109
- Baldwin, J. A., Phillips, M. M., & Terlevich, R. 1981, *PASP*, 93, 5
- Becker, R. H., White, R. L., & Edwards, A. L. 1991, *ApJS*, 75, 1
- Becker, R. H., White, R. L., & Helfand, D. J. 1995, *ApJ*, 450, 559
- Boroson, T. A., & Oke, J. B. 1984, *ApJ*, 281, 535
- Boroson, T. A., & Green, R. F., 1992, *ApJS*, 80, 109
- Brown, J. C., & McLean, I. S. 1977, *A&A*, 57, 141
- Brotherton, M. S. 1996, *ApJS*, 102, 1
- Brotherton, M. S., Wills, B. J., Dey, A., van Breugel, W., & Antonucci, R. 1998, *ApJ*, 501, 110
- Bruzual, A. G., & Charlot, S. 1996, *GISSEL Population Synthesis Models*,
<ftp://gemini.tuc.noao.edu/pub/charlot/bc96>
- Burstein, D. & Heiles, C. 1984, *ApJS*, 54, 33
- Calzetti, D., Kinney, A. L., & Storchi-Bergmann, T. 1994, *ApJ*, 429, 582
- Canalizo, G., & Stockton, A. 1997, *ApJ*, 480, L5
- Cardelli, J. A., Clayton, G. C., & Mathis, J. S. 1989, *ApJ*, 345, 245
- Casali, M. M., & Hawarden, T. G. 1992, *JCMT–UKIRT Newsletter*, 4, 33
- Cimatti, A., Dey, A., van Breugel, W., Antonucci, R., & Spinrad, H. 1996, *ApJ*, 465, 145
- Cid Fernandes, R., & Terlevich, R. 1995, *MNRAS*, 272, 423
- Cohen, M. H., Vermeulen, R. C., Ogle, P. M., Tran, H. D., & Goodrich, R. W. 1997, *ApJ*, 484, 193
- Cohen, M. H., Tran, H. D., Ogle, P. M., & Goodrich, R. W. 1998, in preparation
- Colina, L., & Pérez-Olea, E. 1995, *MNRAS*, 277, 845
- Condon, J. J., Anderson, E., & Broderick, J. J. 1995, *AJ*, 109, 2318
- Condon, J. J., Cotton, W. D., Greisen, E. W., Yin, Q. F., Perley, R. A., Taylor, G. B., & Broderick, J. J. 1998, *AJ*, 115, 1693
- Condon, J. J., Huang, Z.-P, Yin, Q. F., & Thuan, T. X. 1991, *ApJ*, 378, 65

- Cutri, R. M., Huchra, J. P., Low, F. J., Brown, R. L., & Vanden Bout, P. A. 1994, *ApJ*, 424, L65
- Dey, A., & van Breugel, W. 1994, in *Mass-Transfer Induced Activity in Galaxies*, ed. I. Shlosman, (New York: Cambridge University Press), p. 263
- Dey, A., Cimatti, A., van Breugel, W., Antonucci, R., & Spinrad, H. 1996, *ApJ*, 465, 157
- Dopita, M. A., Heisler, C., Lumsden, S., & Bailey, J. 1998, *ApJ*, 498, 570
- Douglas, J. N., Bash, F. N., Bozayan, F. A., Torrence, G. W., & Wolfe, C. 1996, *AJ*, 111, 1945
- Dressler, A., & Gunn, J. E. 1983, *ApJ*, 270, 7
- Francis, P. J., Hewett, P. C., Foltz, C. B., Chaffee, F. H., Weymann, R. J., & Morris, S. L. 1991, *ApJ*, 373, 465
- Genzel, R., Lutz, D., Sturm, E., Egami, E., Kunze, D., Moorwood, A. F. A., Rigopoulou, D., Spoon, H. W. W., Sternberg, A., Tacconi-Garman, L. E., Tacconi, L., & Thatte, N. 1998, *ApJ*, 498, 579
- Goodrich, R. W., & Miller, J. S. 1989, *ApJ*, 346, L21
- Goodrich, R. W., Miller, J. S., Martel, A., Cohen, M., Tran, H. D., Ogle, P. M., & Vermeulen, R. C. 1996, *ApJ*, 456, L9
- Granato, G. L., Danese, L., & Franceschini, A. 1996, *ApJ*, 460, L11
- Gregory, P. C., & Condon, J. J. 1991, *ApJS*, 75, 1011
- Heckman, T. M. 1980, *A&A*, 87, 152
- Heckman, T. M. 1983, *ApJ*, 271, L5
- Heckman, T. M., Gonzalez-Delgado, R., Leitherer, C., Meurer, G. R., Krolik, J., Wilson, A. S., Koratkar, A., & Kinney, A. 1997, *ApJ*, 482, 114
- Heisler, C. A., Lumsden, S. L., & Bailey, J. A. 1997, *Nature*, 385, 700
- Hickson, P., & Hutchings, J. B. 1987, *ApJ*, 312, 518
- Hines, D. C., & Wills, B. J. 1993, *ApJ*, 415, 82
- Hines, D. C., Schmidt, G. D., Smith, P. S., Cutri, R. M., Low, F. J. 1995, *ApJ*, 450, L1
- Hutchings, J. B., & Neff, S. G. 1991, *AJ*, 101, 434
- Jackson, N., & Browne, I. W. A. 1991, *MNRAS*, 250, 414
- Jackson, N., & Tadhunter, C. N. 1993, *A&A*, 272, 105

- Joly, M. 1991, *A&A*, 242, 49
- Kartje, J. F. 1995, *ApJ*, 452, 565
- Kay, L. 1994, in *The First Stromlo Symposium: The Physics of Active Galaxies*, ASP Conference Series Vol. 54, eds. G. V. Bicknell, M. A. Dopita, & P. J. Quinn (San Francisco: Astron. Soc. Pac.), p. 265
- Kim, D.-C., Veilleux, S., & Sanders, D. B. 1998, *ApJ*, in press, astro-ph/9806149
- Kishimoto, M. 1996, *ApJ*, 468, 606
- Kleinmann, S. G., Hamilton, D., Keel, W. C., Wynn-Williams, C. G., Eales, S. A., Becklin, E. E., & Kuntz, K. D. 1988, *ApJ*, 328, 161
- Liu, C. T., & Kennicutt, R. C. 1995, *ApJ*, 450, 547
- Liu, C. T., & Green, R. F. 1996, *ApJ*, 458, L63
- Low, F. J., Huchra, J. P., Kleinmann, S. G., & Cutri, R. M. 1988, *ApJ*, 287, 95
- Lutz, D., Spoon, H. W. W., Rigopoulou, D., Moorwood, A. F. M., & Genzel, R. 1998, *ApJ*, 505, L103
- Matthews, K., & Soifer, B. T. 1994, in *Infrared Astronomy with Arrays: the Next Generation*, ed. I. McLean (Dordrecht: Kluwer Academic Publishers), p. 239
- Miller, J. S., & Goodrich, R. W. 1990, *ApJ*, 355, 456
- Miller, J. S., Goodrich, R. W., & Mathews, W. G. 1991, *ApJ*, 378, 47
- O’Dea, C. P. 1998, *PASP*, 110, 4930
- Oegerle, W. R., Hill, J. M., & Hoessel, J. G. 1991, *ApJ*, 381, L9
- Ogle, P. M., Cohen, M. H., Miller, J. S., Tran, H. D., Fosbury, R. A. E., & Goodrich, R. W. 1997, *ApJ*, 482, L37
- Oke, J. B., Cohen, J. G., Carr, M., Cromer, J., Dingizian, A., Harris, F. H., Labreque, S., Lucinio, R., Schaal, W., Epps, H., & Miller, J. 1995, *PASP*, 107, 375
- Orr, M. J. L., & Browne, I. W. A., 1982, *MNRAS*, 200, 1067
- Osterbrock, D. E. 1977, *ApJ*, 215, 733
- Rengelink, R., Tang, Y., de Bruyn, A., Miley, G., Bremer, M. N., Röttering, H., & Bremer, M. A. R. 1997, *A&A*, 124, 259
- Rowan-Robinson, M., & Crawford, J. 1989, *MNRAS*, 238, 523

- Rowan-Robinson, M., Broadhurst, T., Lawrence, A., McMahon, R. G., Lonsdale, C. J., Oliver, S. J., Taylor, A. N., Hacking, P. B., Conrow, T., Saunders, W., Ellis, R. S., Efstathiou, G. P., & Condon, J. J. 1991, *Nature*, 351, 719
- Salpeter, E. E. 1955, *ApJ*, 121, 161
- Sanders, D. B., Soifer, B. T., Elias, J. H., Madore, B. F., Mathews, K., Neugebauer, G., Scoville, Z. 1988, *ApJ*, 325, 74
- Sanders, D. B., & Mirabel, I. F. 1996, *ARA&A*, 34, 749
- Serkowski, K., Mathewson, D. S., & Ford, V. L. 1975, *ApJ*, 196, 261
- Schaerer, D., & Vacca, W. D. 1998, *ApJ*, 497, 618
- Soifer, B. T. et al. 1987, *ApJ*, 320, 238
- Sopp, H. M., & Alexander, P. 1991, *MNRAS*, 251, 14P
- Stanford, S. A., Stern, D., van Breugel, W., De Breuck, C. 1998, *ApJ*, in preparation
- Stocke, J. T., Morris, S. L., Weymann, J. T., & Foltz, C. B. 1992, *ApJ*, 396, 487
- Stockton, A. 1998, in *Galaxy Interactions at Low and High Redshift*, IAU Symp. 186, eds. D. Sanders & J. Barnes (San Francisco: Astron. Soc. Pac.), in press
- Stockton, A., Canalizo, G., & Close, L. M. 1998, *ApJ*, 500, L121
- Storchi-Bergmann, T., Cid Fernandes, R., & Schmitt, H. R. 1998, *ApJ*, 501, 94
- Surace, J. A., Sanders, D. B., Vacca, W. D., Veilleux, S., & Mazzarella, J. M. 1998, *ApJ*, 492, 116
- Terlevich, R., Tenorio-Tagle, G., Franco, J., & Melnick, J. 1992, *MNRAS*, 255, 713
- Tran, H. D. 1995, *ApJ*, 440, 565
- Tran, H. D., Cohen, M. H., & Goodrich, R. W. 1995, *AJ*, 110, 2597
- Tran, H. D., Filippenko, A. V., Schmidt, G. D., Bjorkman, K. S., Jannuzi, B. T., & Smith, P. S. 1997, *PASP*, 109, 489
- Tran, H. D. 1998, in preparation
- Tran, H. D., Cohen, M. H., Ogle, P. M., Goodrich, R. W., & di Serego Alighieri, S. 1998, *ApJ*, 500, 660
- Veilleux, S., Kim, D.-C., Sanders, D. B., Mazzarella, J. M., & Soifer, B. T. 1995, *ApJS*, 98, 171
- Veilleux, S., Sanders, D. B., & Kim, D.-C. 1997, *ApJ*, 484, 92

- Veilleux, S., & Osterbrock, D. E. 1987, *ApJS*, 63, 295
- Véron-Cetty, M.-P., & Véron, P. 1996, *ESO Sci. Rep.*, 17, 1
- Wills, B. J., Wills, D., Evans, N. J., Natta, A., Thompson, K. L., Breger, M., & Sitko, M. L. 1992, *ApJ*, 400, 96
- Wills, B. J., & Hines, D. C. 1998, in *Mass Ejection from Active Galactic Nuclei*, ASP Conference Series, Vol. 128, eds. N. Arav, I. Shlosman, & R. J. Weymann (San Francisco: Astron. Soc. Pac.), p. 99
- Wilson, A. S., & Tsvetanov, Z. I. 1994, *AJ*, 107, 1227
- Wirth, G. D., Koo, D. C., & Kron, R. G. 1994, *ApJ*, 435, L105
- Young, S., Hough, J. H., Efstathiou, A., Wills, B. J., Bailey, J. A., Ward, M. J., & Axon, D. J. 1996, *MNRAS*, 281, 1206
- Zheng, W., & Keel, W. C. 1991, *ApJ*, 382, 121

Table 1. Infrared Properties

Object	z	m^a	$\log(L_{IR}/L_{\odot})^b$	f_{12}	f_{25}	f_{60}	f_{100}	f_{25}/f_{60}
FF J1614+3234	0.710	19.1	12.6 – 13.2	< 0.065	< 0.055	0.174	< 0.54	< 0.31
TF J1020+6436	0.153	19.0	11.9 – 12.1	< 0.095	< 0.062	0.86	1.24	< 0.072
TF J1736+1122	0.162	18.0	11.8 – 12.3	< 0.081	0.196	0.484	< 3.31	0.404

f_{12} , f_{25} , f_{60} , and f_{100} are the *IRAS* flux densities in units of Jy at 12 μm , 25 μm , 60 μm , and 100 μm (from NASA/IPAC Extragalactic Database).

^aApparent photographic magnitudes from Condon et al. (1995), except for FF J1614+3234, where an r_s magnitude from Stanford et al. (1998) is listed.

^b $L_{IR} \equiv L(8\text{--}1000 \mu\text{m})$ is computed from the observed fluxes in four *IRAS* bands, according to the formulae given in Sanders & Mirabel (1996). The lower value denotes the luminosity that results from setting to zero all bands with upper flux limits, and the upper value is obtained from assuming that these limits are actual detections.

Table 2. Radio Properties

Object	RA (J2000)	Dec (J2000)	S_{365}^a	S_{1400}	S_{4850}	$-\alpha_{1400}^{365}$	$-\alpha_{4850}^{1400}$	$\log R^b$	$\log L_{1400}^c$
FF J1614+3234	16 14 22.11	+32 34 03.7	...	1.19 ± 0.14^d	31.3
TF J1020+6436 ^e	10 20 41.05	+64 36 05.5	1037 ± 40	287 ± 9^g	81.1 ± 0.2	0.96	1.02	2.70	32.2
TF J1736+1122 ^f	17 36 54.92	+11 22 40.0	333 ± 29	122 ± 4^g	35.5 ± 0.2	0.75	0.99	2.34	31.9

Radio flux densities S_ν are in units of mJy; spectral index α is defined for $S_\nu \propto \nu^\alpha$.

^aTexas Sky Survey (Douglas et al. 1996).

^bRatio of 5 GHz radio to optical B band flux, computed using eqs. (1)-(3) of Stocke et al. (1992). The usual dividing line between radio-loud and radio-quiet quasars is $\log R \approx 1$.

^c1.4 GHz radio luminosity in units of $\text{ergs s}^{-1} \text{Hz}^{-1}$. The usual dividing line between radio-loud and radio-quiet quasars is $\log L_{1400} = 32.5$.

^dFIRST Survey (Becker et al. 1995).

^eWENSS flux is 1075 ± 4 mJy at 327 MHz.

^fVLA 8440 MHz flux is 16.6 ± 1.0 mJy (this paper), which implies $\alpha_{8440}^{4850} = -1.45$. Thus the radio spectrum steepens rapidly between 365 MHz and 8440 MHz.

^gNVSS (NRAO VLA Sky Survey; Condon et al. 1998).

Table 3. Emission Line Flux Ratios, Equivalent Widths and FWHMs

Line	TF J1736+1122 ^a			TF J1020+6436 ^a			FF J1614+3234 ^a		
	Flux Ratio ^b	EW ^c	FWHM ^d	Flux Ratio ^{b,e}	EW ^c	FWHM ^d	Flux Ratio ^b	EW ^c	FWHM ^d
C II] λ 2326	0.71	6.2	1390
[Ne V] λ 3346	0.117	8.37	1250						
[Ne V] λ 3426 + O III λ 3444	0.319	23.3	1040						
[O II] λ 3727	2.202	209	1080	2.12 (6.52)	120	620	3.52	57	990
H11 λ 3771	0.00721	0.67	...						
H10 λ 3798	0.0152	1.47	510						
H9 λ 3835	0.0201	1.81	105						
[Ne III] λ 3869 + He I λ 3868	0.699	68.0	895	0.46 (1.3)	20	480	0.62:	10:	...
H8 + He I λ 3889	0.175	17.3	975						
He ϵ λ 3970 + [Ne III] λ 3967	0.328	35.0	950	0.22: (0.55:)	11:	...			
[S II] λ 4071	0.195	22.0	1280	0.14: (0.31:)	6.6:	...			
H δ λ 4102	0.192	21.8	920	0.22: (0.48:)	9.8:	...			
[Fe V] λ 4227	0.0193	2.20	570						
H γ λ 4340	0.389	47.1	870	0.36 (0.62)	17	530	0.78:	15:	...
[O III] λ 4363	0.123	14.8	940	0.19: (0.32:)	9:	...			
He I λ 4471	0.0362	4.75	930						
[Fe III] λ 4658	0.00999	1.23	420						
He II λ 4686n	0.0961	10.9	525	0.13 (0.16)	5.0	240			
WR bump	0.140	20.4	3990						
[Ar IV] λ 4712	0.00804	1.00	...						
[Ar IV] λ 4740	0.0190	2.70	710						
H β (n) λ 4861	1.00	140	870	1.00 (1.00)	36.0	340	1.00	21:	780
[O III] λ 4959	3.357	600.0	840	1.76 (1.61)	63.0	430	0.93	20.0	...
[O III] λ 5007	9.886	1750	820	5.37 (4.71)	186	420	2.01	45.0	860
[Fe VII] λ 5159	0.0659	11.2	2160						
[N II] λ 5200	0.0784	13.4	790	0.35 (0.26)	11	450			
[Fe III] λ 5270	0.0239	4.2	675						
He II λ 5412	0.0158	3.1	600						
[Cl III] $\lambda\lambda$ 5518, 5538	0.0248	5.17	...						
[Fe VII] λ 5721	0.0240	5.20	1420						
[N II] λ 5755	0.0358	7.80	1000	0.13 (0.067)	2.7	...			
He I λ 5876	0.177	38.6	...	0.22 (0.11)	4.5	150			
He II λ 6074 + [Fe VII] λ 6087	0.0401	9.31	1270						
[O I] λ 6300	0.579	123.5	880	1.74 (0.70)	32.7	260			
[O I] λ 6364	0.199	42.5	895	0.57 (0.22)	10.6	260			
[N II] λ 6548	0.951	230	1090	3.60 (1.30)	70.0	400			
H α (n) λ 6563	2.89	700.0	725	8.77 (3.10)	171	240			
H α (b) λ 6563	0.882	214	5580						
[N II] λ 6583	2.607	630	1170	10.8 (3.84)	211	450			
He I λ 6678	0.0888	21.8	1330						
[S II] λ 6716	0.469	120	740	3.09 (1.02)	47.6	250			
[S II] λ 6731	1.161	280	1010	2.68 (0.88)	41.1	250			
[Ar V] λ 7006?	0.0236	5.8	...						
He I λ 7065	0.0515	11.9	865						
[Ar III] λ 7136	0.277	62.0	1130	0.28 (0.076)	4.1	...			
[O II] $\lambda\lambda$ 7320, 7330	0.315	64.0	1140	0.99 (0.26)	13	...			
[Ni II] λ 7378	0.0372	7.4	550						
[Fe II] λ 7453	0.0601	12.2	1090						

^aFlux ratios and EWs are measured from starlight-subtracted spectrum.

^bObserved line flux ratios relative to H β ; colon denotes uncertainty \gtrsim 20%.

^cRest-frame equivalent widths in Å.

^dFWHMs (km s⁻¹) have been corrected for instrumental resolution of 550 km s⁻¹.

^eNumbers in parentheses denote values after correction for reddening $E(B - V) = 1.05$, based on the observed Balmer decrement H α /H β = 8.77.

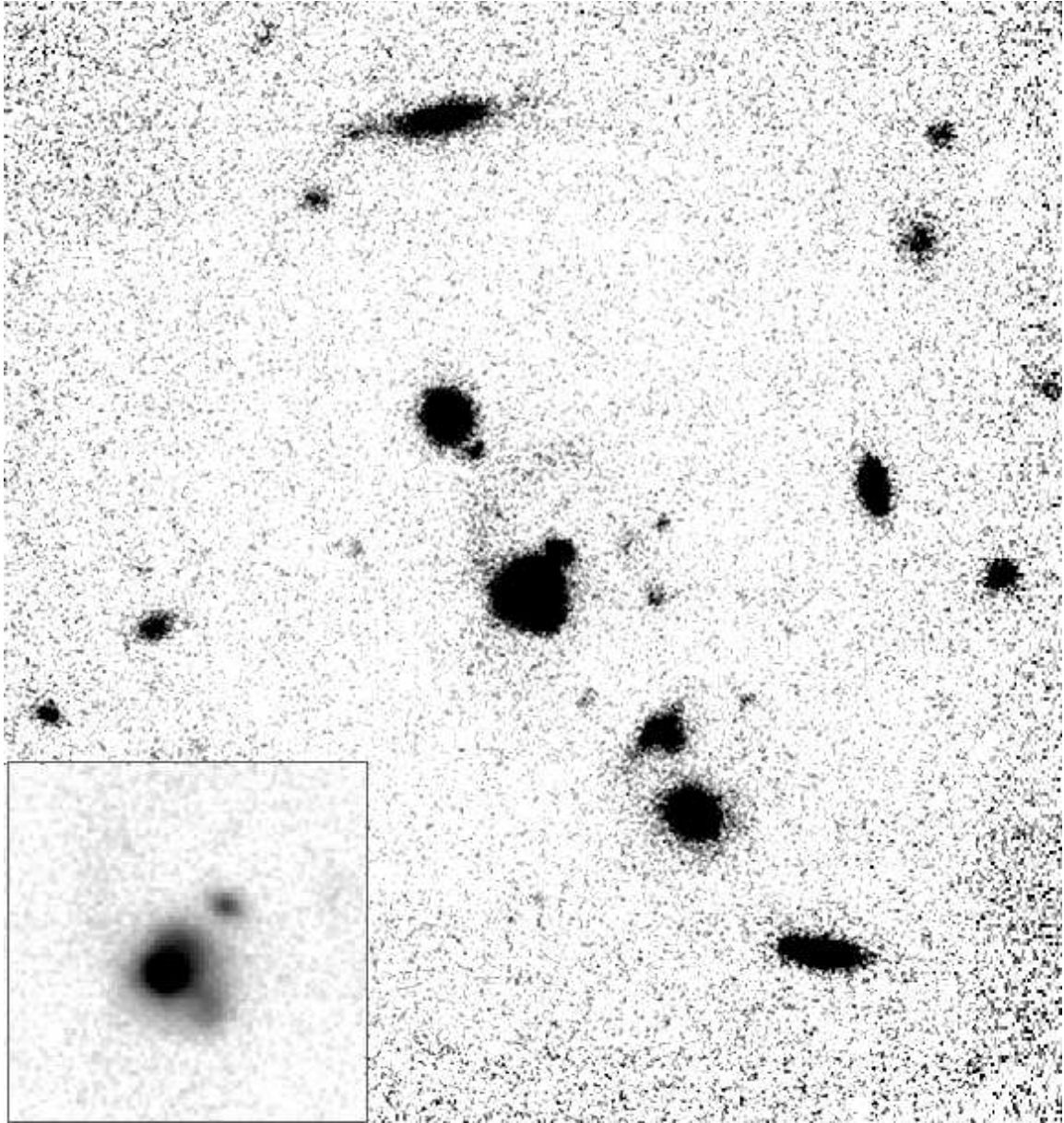


Fig. 1.— K_s -band image of the field of FF J1614+3234 obtained with the W. M. Keck I Telescope. North is up and east is to the left. FF J1614+3234 is centered on the image. The inset displays a $10'' \times 10''$ region centered on FF J1614+3234 at a lower stretch, showing emission extending $1''.8$ to the south-west. Also apparent are a companion $2''.2$ to the northwest and low-level filamentary extensions to the north.

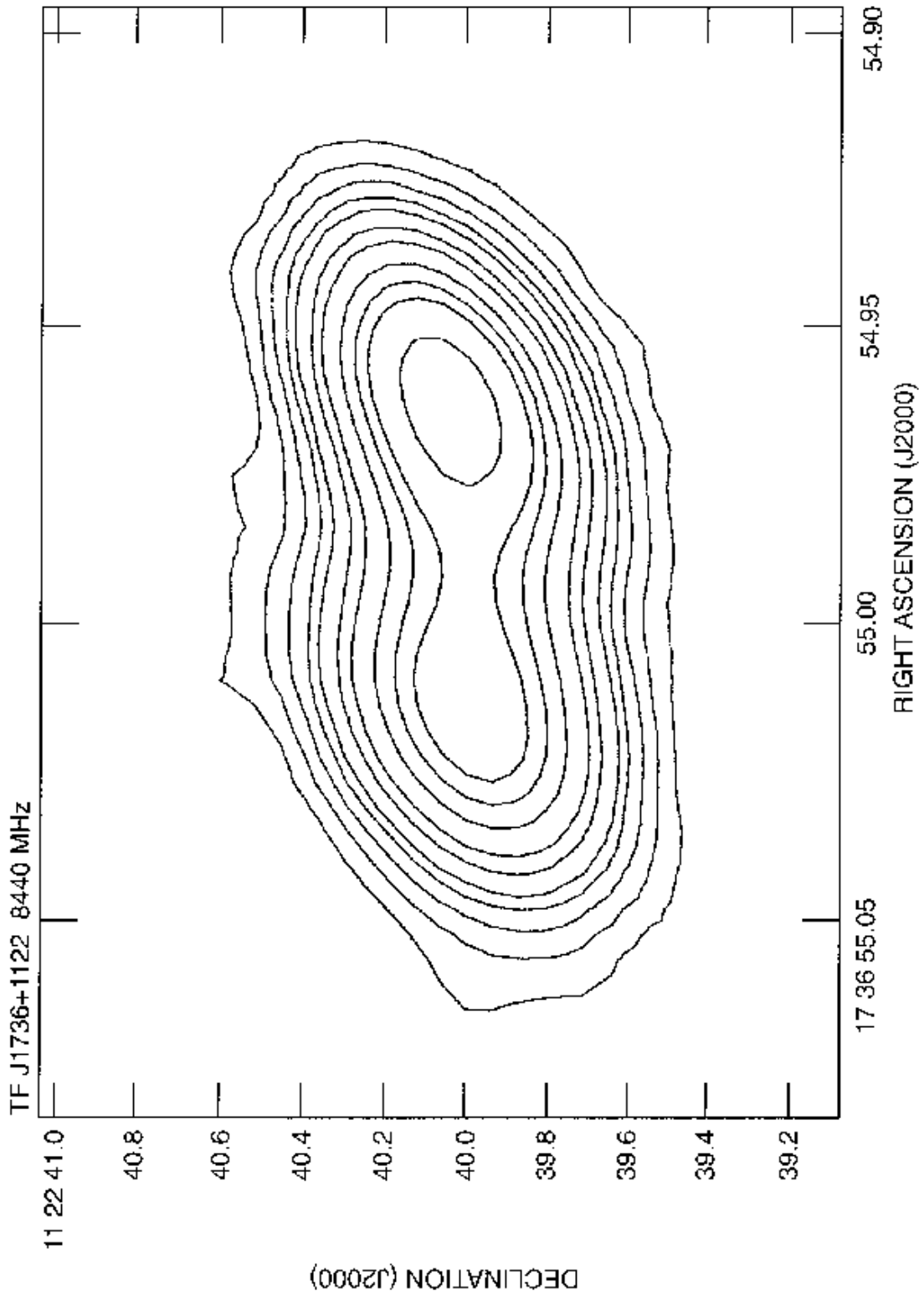


Fig. 2.— The 8440 MHz VLA map of TF J1736+1122. The contour levels are: $0.04 \times (3, 6, 10, 15, 20, 30, 40, 60, 80, 100, 150)$ mJy beam⁻¹. The peak flux is at 7.77×10^{-3} Jy.

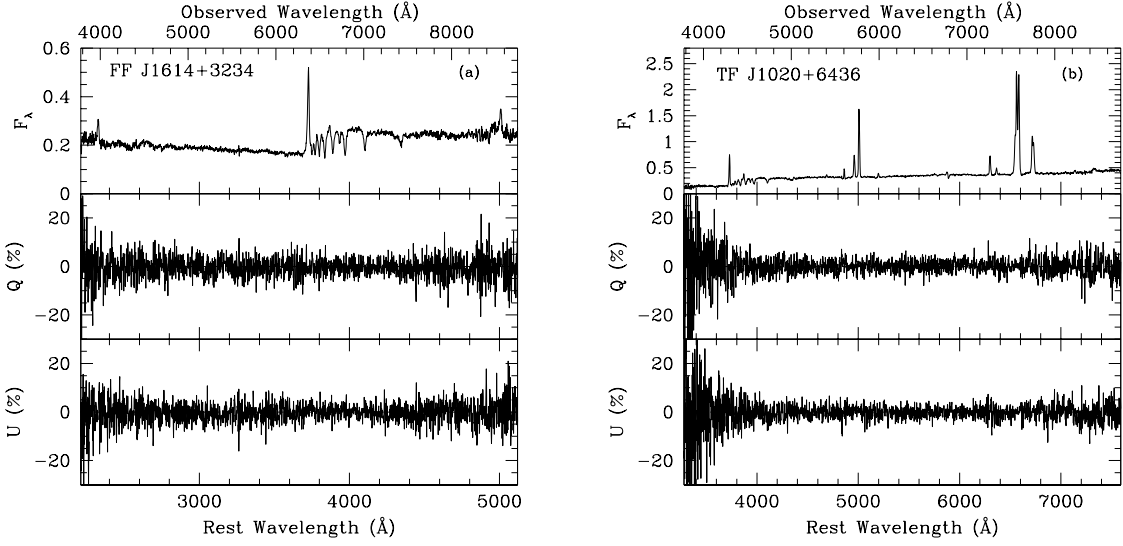


Fig. 3.— Optical spectra and normalized Q and U Stokes parameters for (a) FF J1614+3234 and (b) TF J1020+6436 obtained at the W. M. Keck II Telescope. The flux scales are in units of 10^{-16} ergs cm^{-2} s^{-1} \AA^{-1} . Note the strong Balmer absorption lines characteristic of young stars in the spectra. No significant polarization is detected.

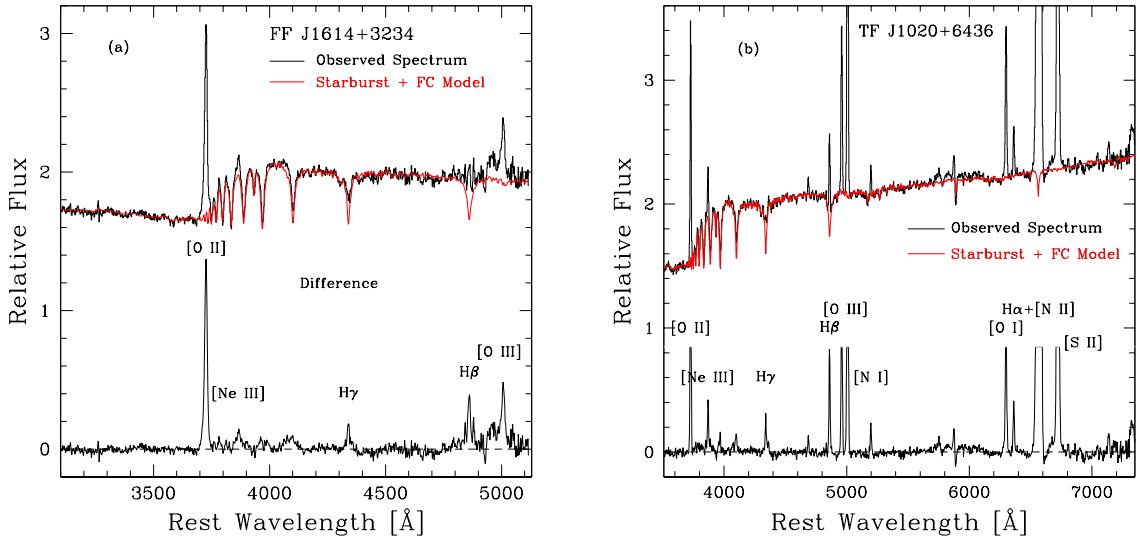


Fig. 4.— Fits of BC96 models to the spectra of (a) FF J1614+3234 and (b) TF J1020+6436. Note the appearance of emission lines of $[\text{Ne III}] \lambda 3869$, $\text{H}\delta$, $\text{H}\gamma$, and $\text{H}\beta$ after removal of the young starburst component.

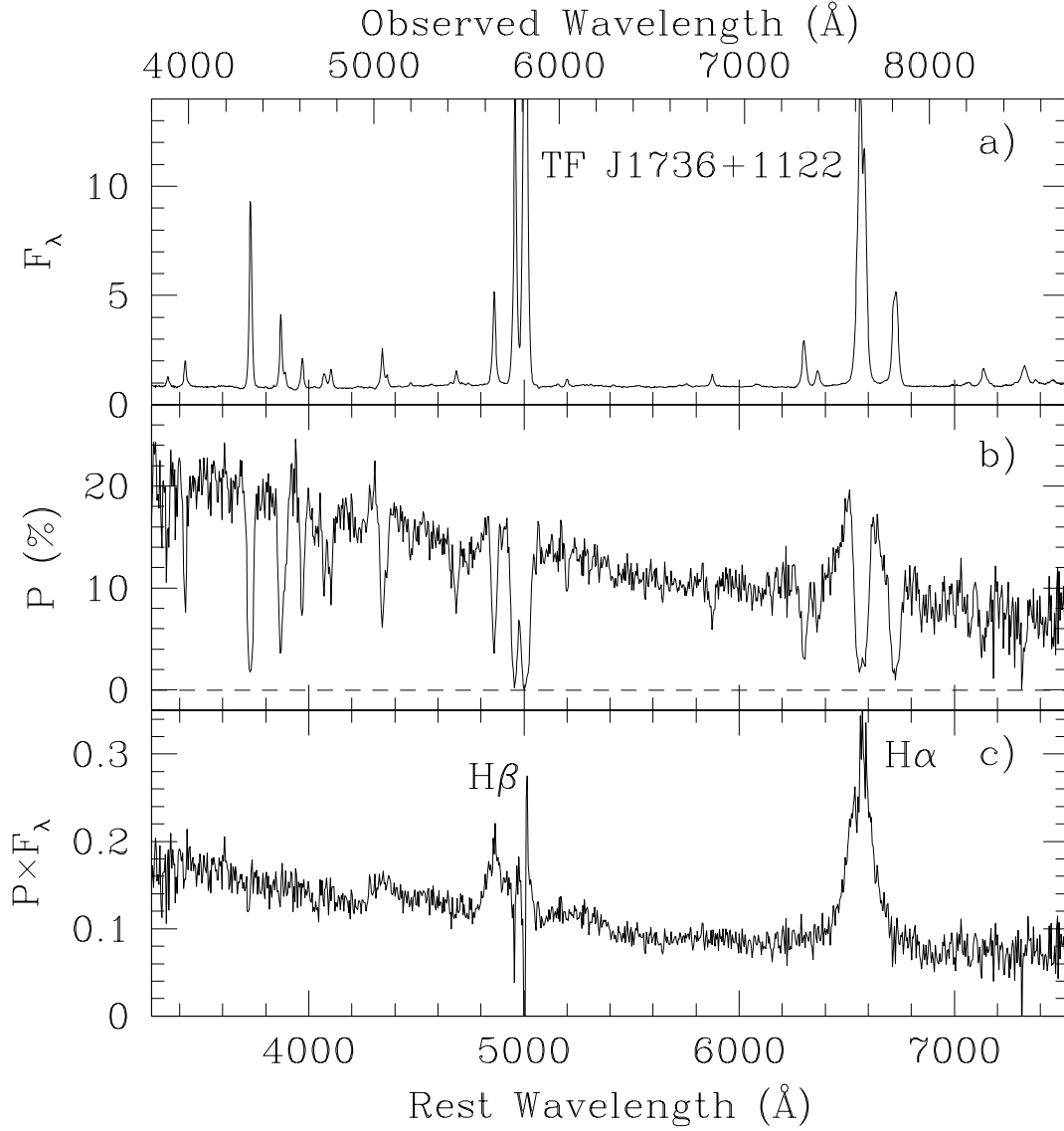


Fig. 5.— Spectropolarimetry of TF J1736+1122. (a) Total flux spectrum F_λ , (b) observed degree of polarization P , and (c) polarized flux spectrum $P \times F_\lambda$. The flux scales are in units of 10^{-16} ergs $\text{cm}^{-2} \text{s}^{-1} \text{\AA}^{-1}$. Fe II emission features are clearly present in $P \times F_\lambda$ around 4570 \AA and 5250 \AA .

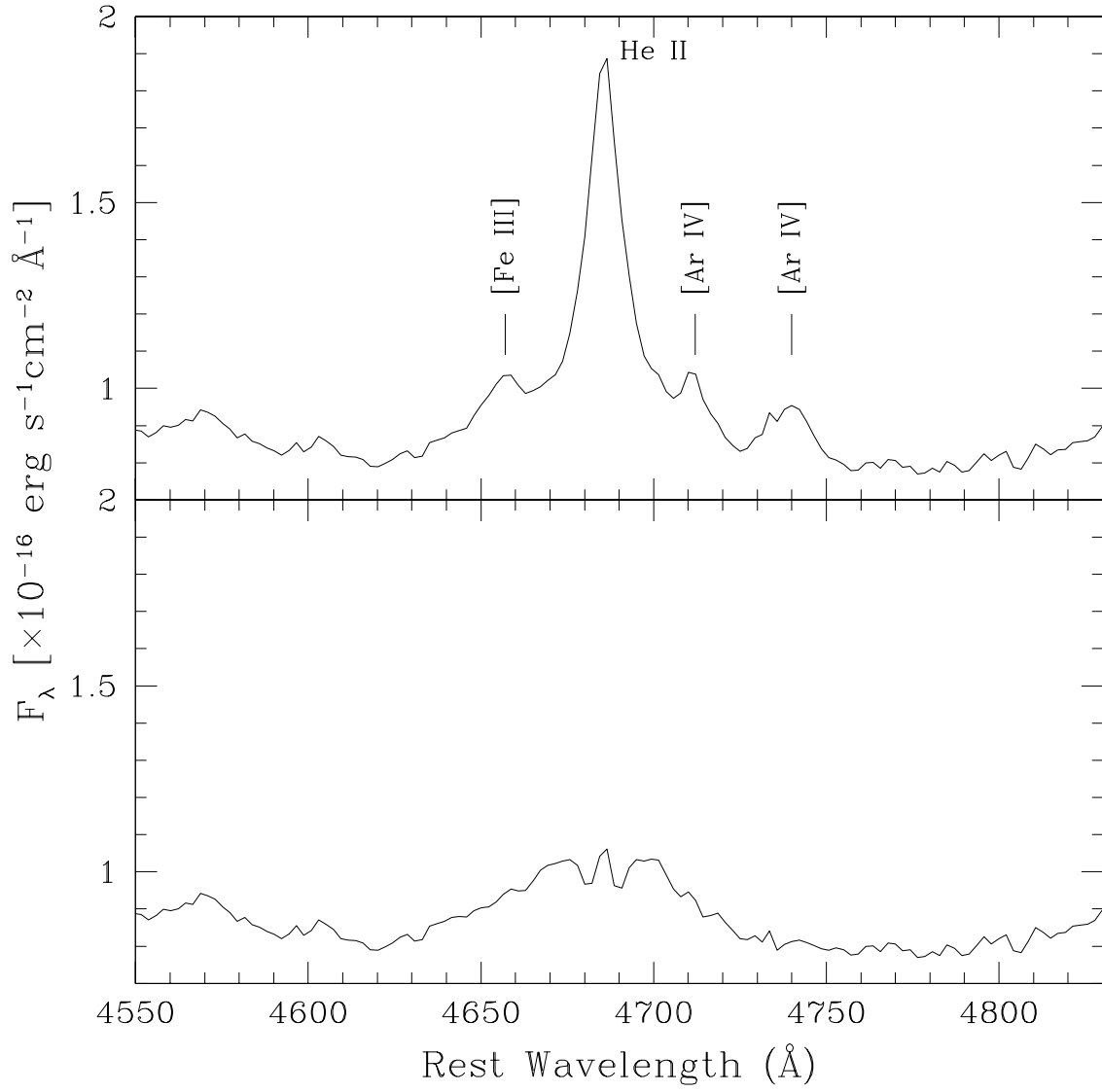


Fig. 6.— Spectrum of TF J1736+1122 showing the W-R bump underlying He II $\lambda 4686$.

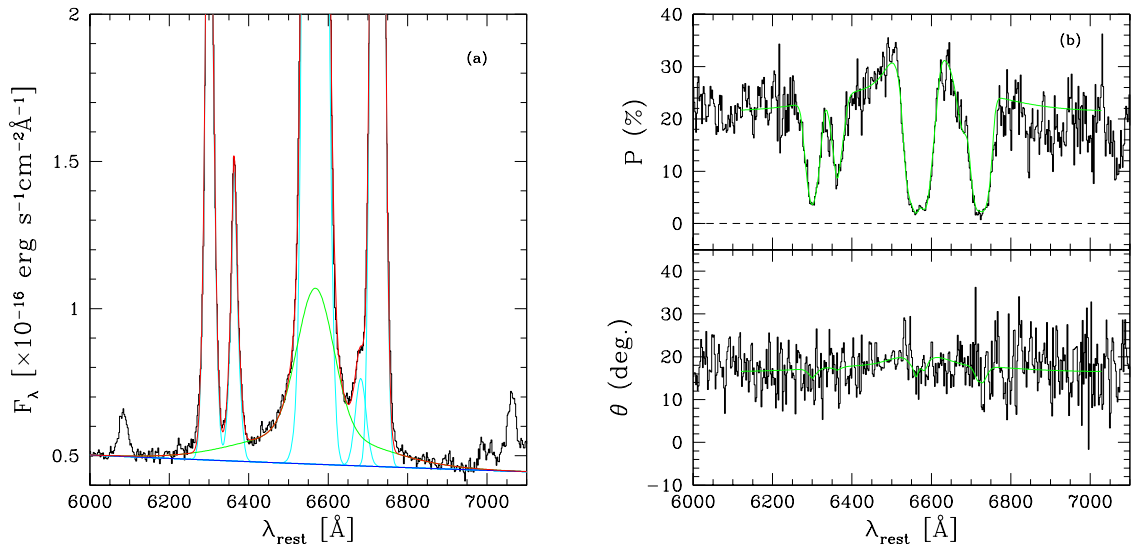


Fig. 7.— Polarization modelling at H α for TF J1736+1122. (a) Fitting of continuum and Gaussian components to emission lines in total flux; (b) Results of the fit (smooth curves) compared to the observed P & θ . The polarization has been corrected for starlight dilution.

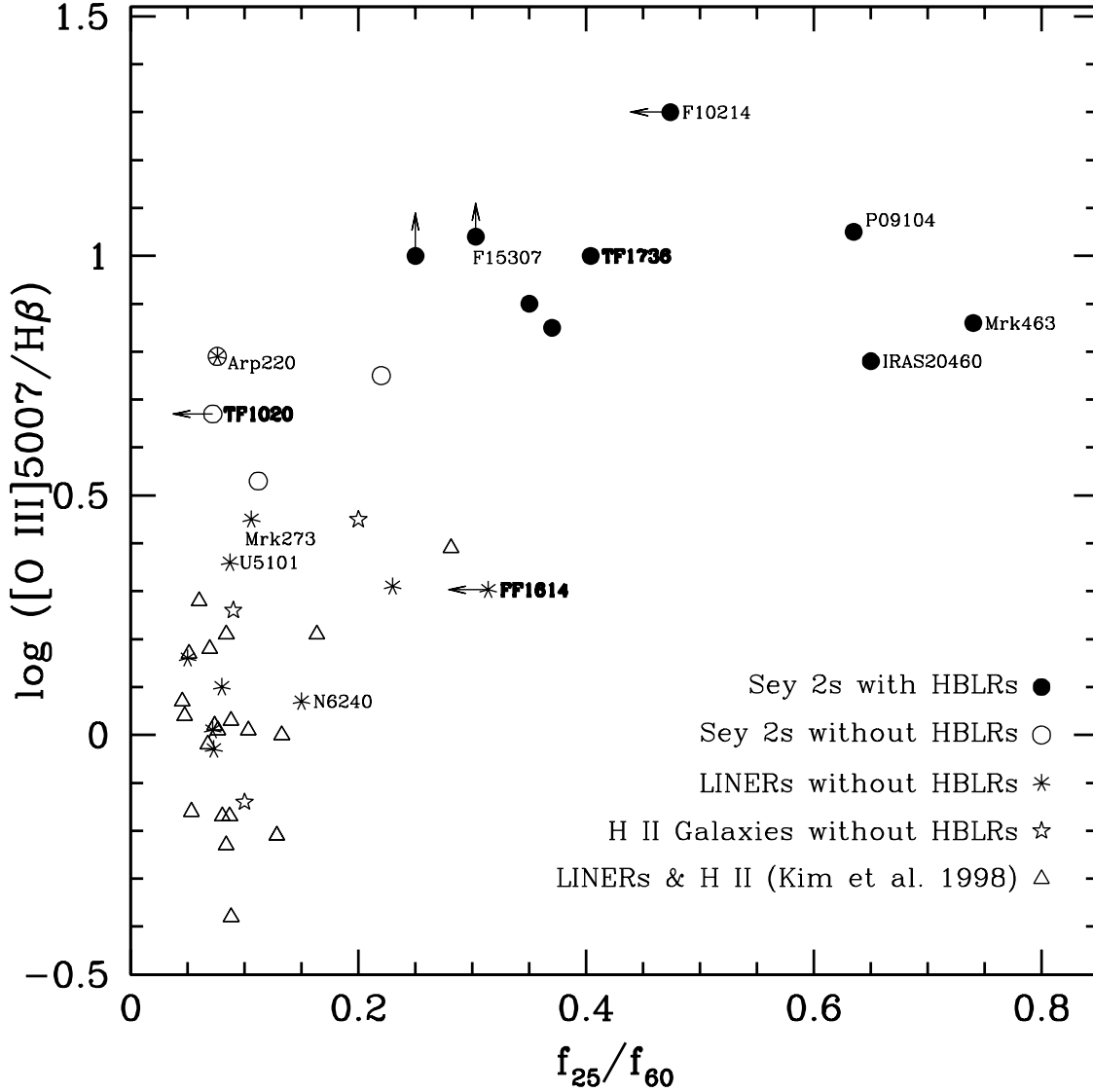


Fig. 8.— $[\text{O III}] \lambda 5007 / \text{H}\beta$ versus IR color f_{25}/f_{60} for narrow-line ULIRGs in which HBLRs have been searched for. Seyfert 2s with HBLRs detected either with spectropolarimetry or near-IR spectroscopy are represented by solid circles. Those without detections of HBLRs are shown as open circles. Stars represent H II region galaxies and asterisks denote LINERs. Also plotted in open triangles are all ULIRGs classified as H II and LINERs in Kim et al. (1998). Note the clear tendency for ULIRGs with HBLRs to have warmer IR color and higher excitation spectrum. The opposite holds for LINERs and H II galaxies.